

ARTICLE

Evaluation of drug–drug interaction potential for pemigatinib using physiologically based pharmacokinetic modeling

Tao Ji | Xuejun Chen | Swamy Yeleswaram

Incyte Research Institute, Wilmington, Delaware, USA

Correspondence

Swamy Yeleswaram, Incyte Research Institute, 1801 Augustine Cut-off, Wilmington, DE 19803, USA.
Email: yeleswaram@incyte.com

Funding information

The study was funded by Incyte Corporation, Wilmington, DE, USA.

Abstract

Pemigatinib is a potent inhibitor of fibroblast growth factor receptor being developed for oncology indications. It is primarily metabolized by cytochrome P450 (CYP) 3A4, and the ratio of estimated concentration over concentration required for 50% inhibition ratio for pemigatinib as an inhibitor of P-glycoprotein (P-gp), organic cation transporter-2 (OCT2), and multidrug and toxin extrusion protein-1 (MATE1) exceeds the cutoff values established in regulatory guidance. A Simcyp minimal physiologically based pharmacokinetic (PBPK) with advanced dissolution, absorption, and metabolism absorption model for pemigatinib was developed and validated using observed clinical pharmacokinetic (PK) data and itraconazole/rifampin drug–drug interaction (DDI) data. The model accurately predicted itraconazole DDI (approximate 90% area under the plasma drug concentration–time curve [AUC] and approximate 20% maximum plasma drug concentration [C_{\max}] increase). The model underpredicted rifampin induction by 100% (approximate 6.7-fold decrease in AUC and approximate 2.6-fold decrease in C_{\max} in the DDI study), presumably reflecting non-CYP3A4 mechanisms being impacted. The verified PBPK model was then used to predict the effect of other CYP3A4 inhibitors/inducers on pemigatinib PK and pemigatinib as an inhibitor of P-gp or OCT2/MATE1 substrates. The worst-case scenario DDI simulation for pemigatinib as an inhibitor of P-gp or OCT2/MATE1 substrates showed only a modest DDI effect. The recommendation based on this simulation and clinical data is to reduce pemigatinib dose for coadministration with strong and moderate CYP3A4 inhibitors. No dose adjustment is required for weak CYP3A4 inhibitors. The coadministration of strong and moderate CYP3A4 inducers with pemigatinib should be avoided. PBPK modeling suggested no dose adjustment with P-gp or OCT2/MATE1 substrates.

This is an open access article under the terms of the [Creative Commons Attribution-NonCommercial-NoDerivs](https://creativecommons.org/licenses/by-nc-nd/4.0/) License, which permits use and distribution in any medium, provided the original work is properly cited, the use is non-commercial and no modifications or adaptations are made.

© 2022 The Authors. *CPT: Pharmacometrics & Systems Pharmacology* published by Wiley Periodicals LLC on behalf of American Society for Clinical Pharmacology and Therapeutics.

Study Highlights

WHAT IS THE CURRENT KNOWLEDGE ON THE TOPIC?

Based on in vitro and clinical data, pemigatinib is a substrate of cytochrome P450 (CYP) 3A4 and an inhibitor of P-glycoprotein (P-gp) or organic cation transporter-2 (OCT2)/multidrug and toxin extrusion protein-1 (MATE1). Therefore, perpetrators of CYP3A4 could alter its metabolism and cause changes in pemigatinib exposure, and pemigatinib may change the exposure of P-gp or OCT2/MATE1 substrates.

WHAT QUESTION DID THIS STUDY ADDRESS?

This study developed a physiologically based pharmacokinetic (PBPK) model for pemigatinib to predict the drug–drug interaction (DDI) for other CYP3A4 inhibitors/inducers or substrates of P-gp or OCT2/MATE1 to support the label and provide dose recommendations for clinical trials.

WHAT DOES THIS STUDY ADD TO OUR KNOWLEDGE?

This study demonstrated the value of using PBPK modeling to assess the clinical DDI risk of pemigatinib. Whereas the model used accurately predicted itraconazole DDI, a limitation of this study is that the model underpredicted rifampin induction by 100%. Despite this, the modeling and simulation confirmed that pemigatinib is primarily metabolized by CYP3A4 and provided dose recommendations for pemigatinib when coadministered with CYP3A4 inhibitors/inducers.

HOW MIGHT THIS CHANGE DRUG DISCOVERY, DEVELOPMENT, AND/OR THERAPEUTICS?

The validated PBPK model using clinical data can be used to evaluate clinical DDI potential where the clinical data lack and to inform the dose recommendation.

INTRODUCTION

Pemigatinib is an inhibitor of the fibroblast growth factor receptor (FGFR) family of receptor tyrosine kinases that is proposed for the treatment of malignant diseases or other diseases related to FGFR dysregulation.¹ Pemigatinib has been approved by the US Food and Drug Administration,² European Medicines Agency,³ and Japanese Ministry of Health, Labor, and Welfare⁴ and conditionally approved by Health Canada⁵ for the treatment of adults with previously treated, unresectable locally advanced or metastatic cholangiocarcinoma with an FGFR2 fusion or other rearrangement.

Pemigatinib is a Biopharmaceutics Classification System Class II compound with high permeability and pH-dependent solubility. In vitro transport studies indicate that pemigatinib is a substrate of both P-glycoprotein (P-gp) and breast cancer resistance protein (data on file); however, the efflux mediated by P-gp and breast cancer resistance protein was saturated at concentrations of 1 and 30 μ M, respectively, in vitro, suggesting that no drug–drug interactions (DDIs) are expected at clinically relevant exposures (e.g., for the recommended pemigatinib dose of 13.5 mg orally once daily [q.d.], geometric mean [coefficient of variation percent] steady-state [SS] $AUC_{0-24h} = 2620 \text{ nM} \cdot \text{h}$ [54%]; maximum plasma drug

concentration [C_{max}] = 236 nM [56%]).⁶ Data from in vitro studies have indicated that cytochrome P450 (CYP) 3A4 is the major isozyme responsible for the metabolism of pemigatinib. In addition, pemigatinib is an inhibitor of P-gp, organic cation transporter-2 (OCT2), and multidrug and toxin extrusion protein-1 (MATE1).

Pemigatinib exhibited an approximately linear relationship for both C_{max} and area under the concentration–time curve (AUC) following oral dosing over the dose range studied in the first-in-human dose-escalation and cohort-expansion study conducted in patients with cancer (1–20 mg).⁶ Pemigatinib was rapidly absorbed with a terminal half-life of ~15 h. The recommended dose is 13.5 mg q.d. on a 2-weeks-on/1-week-off therapy schedule and 13.5 mg q.d. on a continuous schedule. At the 13.5-mg q.d. dose, the geometric mean SS C_{max} value was 236 nM, and the geometric mean area under the plasma concentration versus time curve at steady-state, over one dosing interval ($AUC_{ss,0-24}$) value was 2620 nM · h. Pemigatinib exhibited a low SS oral clearance with a geometric mean of 9.88–11.7 L/h and a moderate apparent volume of distribution with geometric mean of 173–244 L. The effect of food on pemigatinib plasma exposures in patients with cancer was modest and not clinically meaningful. In the fed state, median time taken to reach C_{max} was delayed to 4.0 h postdose. The

geometric mean of C_{max} decreased by 18%, and the geometric mean of AUC over the dosing interval (τ) at SS (AUC_{0-24}) increased by 11%. A mass balance study showed that 12.6% and 82.4% of the total radioactivity was excreted in urine and feces of healthy participants, respectively (unpublished data). The oral absorption of pemigatinib was nearly complete, based on feces metabolite profiling. Renal excretion of pemigatinib was low (~1%), and liver metabolism is inferred to be the major clearance pathway for pemigatinib. A DDI study showed an approximate 90% increase in pemigatinib AUC with itraconazole coadministration and an 85% decrease in AUC with rifampin coadministration.⁷ The DDI study with acid-reducing agents showed that the geometric mean C_{max} and AUC of pemigatinib decreased by 35% and 8%, respectively, upon coadministration with proton pump inhibitor, esomeprazole; the geometric mean C_{max} and AUC of pemigatinib decreased by 2% and increased by 3%, respectively, upon coadministration with the histamine-2 antagonist ranitidine.

The ratio of intestinal luminal concentration estimated as dose in 250 ml/half = maximal inhibitory concentration (IC_{50}) for P-gp and unbound C_{max}/IC_{50} for OCT2 and MATE1 is larger than 10, 0.1, and 0.02, respectively, and these values have exceeded the cutoff values proposed by the US Food and Drug Administration DDI guidance.⁸ Therefore, a physiologically based pharmacokinetic (PBPK) model was used to evaluate pemigatinib as an inhibitor of gut P-gp, OCT2, or MATE1.

The PBPK models that have been validated with observed clinical pharmacokinetic (PK) and DDI data can be used to predict the outcome for other DDI scenarios. The simulation results can also be used to support dose adjustment and label statements. The aim of this modeling and simulation study was to develop a PBPK model for pemigatinib using in silico, in vitro, and clinical data to predict the DDI.

METHODS

Modeling strategy

The Simcyp Population-Based Simulator Version 17 release 1 was used for all simulations (Simcyp). The physicochemical parameters of pemigatinib were measured by Incyte Corporation. The predictions of plasma drug concentration–time profiles and DDI for healthy volunteers and patients with cancer were performed in the Simcyp Simulator using the default Sim-Healthy Volunteer population and Sim-Cancer population, respectively.

The PBPK model for pemigatinib was built and verified using a mixed “bottom-up” and “top-down” approach using parameters from in silico calculation, in

vitro experiments (“bottom-up”) and using in vivo clinical data (“top-down”) to bridge in vitro–in vivo translation. For research purposes, model workspace files are available at the following link: <https://members.simcyp.com/account/globalHealthRepository>; model data set files are available as the following Supplementary Tables: Table S1 (Cohort 1 INCB054828 alone), Table S2 (Cohort 1 INCB05828 + itraconazole), Table S3 (Cohort 2 INCB054828 alone), and Table S4 (Cohort 2 INCB05828 + itraconazole).

Pemigatinib PBPK model

The initial PBPK model for pemigatinib was built using in vitro and in silico data. Data from in vitro studies have indicated that CYP3A4 is the major isozyme responsible for the metabolism of pemigatinib (data on file). Based on mass balance and metabolite identification, the oral absorption of pemigatinib is inferred to be nearly complete (1.4% of the administered radioactive dose was recovered as unchanged pemigatinib in feces), observed renal excretion is low (~1.0% of the dose was excreted in urine as unchanged pemigatinib), and liver metabolism is inferred to be the major clearance pathway for pemigatinib. Therefore, a minimal PBPK with advanced dissolution, absorption, and metabolism (ADAM) absorption model for pemigatinib that incorporates CYP3A4-mediated metabolism derived from in vitro data and human absorption, distribution, metabolism, and excretion (ADME) data was then further developed, and the model was used to describe the clinical PK data from pemigatinib-alone cohorts in the CYP3A4-mediated DDI study⁷ and the PK data from the dose groups of 6–20 mg in the phase I dose-escalation and dose-expansion study (NCT02393248).⁶ The sensitivity analysis of the pemigatinib fraction of drug metabolized by CYP3A4 ($f_{mCYP3A4}$) on drug interaction with itraconazole (CYP3A4-mediated DDI study) suggested that CYP3A4 contributes ~55% of the metabolic clearance for pemigatinib. The verified pemigatinib model was then used to simulate the observed effect of itraconazole on pemigatinib PK and to confirm the contribution of CYP3A4 ($f_{mCYP3A4} = 55\%$) to pemigatinib metabolic clearance.

Application of pemigatinib PBPK model

1. Prospective prediction of other strong, moderate, and weak CYP3A4 inhibitors or inducers: the final pemigatinib PBPK model was prospectively applied to estimate the effect of other strong, moderate, and weak CYP3A4 inhibitors or inducers. The simulation results were used for drug label and dose optimization in clinical trials.

2. Evaluation of pemigatinib as an inhibitor of gut P-gp, OCT2, or MATE1 substrates: a sensitivity analysis of pemigatinib P-gp inhibitor constant (K_i) value on the exposures of digoxin (a P-gp substrate) and a worst-case scenario simulation for the interaction between pemigatinib (20 mg q.d., highest dose evaluated in clinical trials, and assuming 10-fold lower measured in vitro K_i values) and metformin (a OCT2/MATE1 substrate) were used to evaluate the effect of pemigatinib as an inhibitor of gut P-gp or OCT2/MATE1 substrates.

Input data for pemigatinib PBPK model

The parameters for the pemigatinib PBPK model are shown in Table 1. Simcyp default values are used for all other parameters in the model.

Pemigatinib is a diprotic base with pKa of 5.7 and 3.1, and the logP value for pemigatinib is 2.2. Pemigatinib primarily binds to albumin and the in vitro fraction of unbound pemigatinib in human plasma is 0.094. The measured blood/plasma value is 0.96, which is similar to the radioactivity blood/plasma value (0.80) determined in

TABLE 1 Summary of key input parameters for the pemigatinib physiologically based pharmacokinetic model

Parameters	Value	Reference/data source
Molecular weight (g/mol)	487.5	Experimental data
logP	2.2	Experimental data
Compound type	Diprotic base	Experimental data
pK _a	5.7, 3.1	Experimental data
B/P	0.96	Experimental data
f _u	0.094	Experimental data
$P_{\text{eff,caco-2}}$ [10^{-6} cm/s]	11.0	Experimental data
Reference $P_{\text{eff,caco-2}}$ [10^{-6} cm/s] (metoprolol)	15.0	Experimental data
Predicted $P_{\text{eff,man}}$ ($\times 10^{-4}$ cm/s)	3.01	Predicted from Caco-2 transport data after calibration
Solubility-pH profile	0.71, 0.65, 0.20, 0.03, 0.001, and 0.001 mg/ml at pH 1.2, 2.0, 3.3, 4.3, 5.3, 6.5, and 7.4	Experimental data
Precipitation model	Model 2	
V_{ss} (L/kg)	2.84 (method 2)	Optimized from clinical PK data for pemigatinib alone cohorts (CYP3A4-mediated DDI study) and adjusted K_p scalar to match the PK data
K_p scalar	4.58	
V_{sac} (L/kg)	1.87	Optimized from clinical PK data for pemigatinib alone cohort (CYP3A4-mediated DDI study)
Q_{sac} (L/h)	44.0	Optimized from clinical PK data for pemigatinib alone cohort (itraconazole DDI study)
$\text{CL}_{\text{int,CYP3A4}}$ ($\mu\text{l}/\text{min}/\text{pmol}$)	0.172	Calculated using Simcyp retrograde model to achieve f_{mCYP3A4} of 55% of total CL_{PO} (14.5 L/h for pemigatinib alone cohorts in itraconazole DDI study)
Additional $\text{CL}_{\text{int-HLM}}$ ($\mu\text{l}/\text{min}/\text{mg}$ protein)	19.2	Calculated using Simcyp retrograde model, entered as HLM CL_{int} under additional CL
CL_{R} (L/h)	0.2	Human mass balance study (unpublished data)
K_i P-gp (μM)	4.8	Experimental data
K_i OCT2 (μM)	0.075	Experimental data
K_i MATE1 (μM)	1.1	Experimental data

Abbreviations: B/P, blood/plasma ratio; CL_{int} , intrinsic metabolic clearance; CL_{PO} , clearance observed for oral administration; CL_{R} , renal clearance; CYP3A4, cytochrome P450 3A4; DDI, drug–drug interaction; f_{mCYP3A4} , fraction of drug metabolized by CYP3A4; f_u, fraction unbound; HLM, human liver microsomes; K_i , inhibitor constant; K_p , ratio of concentration of compound in tissue to compound in plasma at steady state; MATE1, multidrug and toxin extrusion protein –1; OCT2, organic cation transporter –2; $P_{\text{eff,caco-2}}$, Caco-2 cell effective permeability; $P_{\text{eff,man}}$, effective human intestinal permeability; P-gp, P-glycoprotein; PK, pharmacokinetics; Q_{sac} , intercompartmental clearance of single-adjusted compartment; V_{sac} , volume of single-adjusted compartment; V_{ss} , volume of distribution at steady state.

a human ADME study. Pemigatinib exhibits a high apparent permeability value (11×10^{-6} cm/s) at 50 μ M across the Caco-2 monolayer. A high fraction of intestinal absorption (F_a) value of 0.96 was predicted from the ADAM model. The predicted F_a is comparable with the F_a estimated (near complete absorption) from the human ADME data. The solubility of pemigatinib at 37°C is ~0.71 mg/ml in pH 1.2 buffer, 0.65 mg/ml in pH 2.0 buffer, <0.001 mg/ml in pH 6.5 buffer, and <0.001 mg/ml in pH 7.4 buffer. These solubility data were used in the ADAM model.

The minimal PBPK model was used to describe the PK profiles of pemigatinib and the volume of distribution at SS (V_{ss}) was predicted by Method 2 in the PBPK model. The V_{ss} value in the PBPK model was obtained using parameter estimation on the tissue to plasma partition coefficient (K_p) scalar to match the observed clinical PK data from the pemigatinib-alone cohorts in the CYP3A4-mediated DDI study. The K_p scalar of 4.58 was estimated to obtain V_{ss} of 2.84 L/h to fit the PK profile. In addition, parameter estimation was used to obtain the volume of the single-adjusting compartment (1.87 L/kg) and inter-compartmental clearance of the single-adjusting compartment (44.0 L/h) by fitting the observed PK profile.

The in vitro studies and a human ADME study have indicated that CYP3A4 is the major isozyme responsible for the metabolism of pemigatinib. The renal clearance of pemigatinib is ~0.2 L/h. Hepatic clearance through the CYP3A4 enzyme, CYP3A4 intrinsic clearance (CL_{int} ; 0.172 μ l/min/pmol), was estimated using the Simcyp retrograde calculator based on CL_{po} observed in the pemigatinib-alone cohort of the itraconazole DDI study (14.5 L/h)⁷ and predicted F_a (0.96) and predicted fraction of drug entering enterocytes and escaping the first-pass gut wall metabolism (F_g ; 0.93) when $f_{mCYP3A4}$ was assigned as 55%. The $f_{mCYP3A4}$ value in the PBPK model was confirmed by matching predicted pemigatinib PK profiles when administered concomitantly with itraconazole to the clinical observed data from the CYP3A4-mediated DDI study. Patients with cancer in the phase I dose-escalation and dose-expansion study⁶ showed similar CL_{po} (12.0 L/h) as healthy volunteers.⁹

The bidirectional transport ratio of digoxin decreased in the presence of pemigatinib in a concentration-dependent manner with IC_{50} of 4.8 μ M. Pemigatinib inhibited the OCT2 and MATE1 with estimated IC_{50} of 0.075 and 1.1 μ M, respectively.

Simulations

All of the simulations were conducted using a 10×10 design (10 trials with 10 participants per trial) to simulate population variability. Visual checks of the predicted concentration–time profiles were performed, and the

key PK parameters (AUC and C_{max}) were compared. The model was considered to be acceptable when the ratio of the predicted observed parameter was not outside the range of 0.5- to 2-fold.¹⁰

PBPK model development and validation

The pemigatinib PBPK model was validated by simulations of DDIs between pemigatinib and itraconazole or rifampin using a Simcyp virtual healthy volunteer population, with the study design matching the corresponding clinical DDI study in healthy volunteers.⁷ The itraconazole capsule (200 mg) was administered daily from Day 1 to Day 11, and a single 4.5-mg dose of a pemigatinib tablet was administered orally with itraconazole on Day 5. The rifampin capsule (600 mg) was administered daily from Day 1 to Day 12, and a single 13.5-mg dose of a pemigatinib tablet was administered orally with rifampin on Day 8. The simulations were performed using an age range of 18–55 years (proportion of female volunteers: 0.5), matching the demographics of the clinical DDI study in healthy volunteers (Cohort 1 [itraconazole]: median age, 34.5 years [range, 24–50 years]; male, 56%; White, 83%; mean body mass index [BMI], 26.8 kg/m² [SD, 3.09]; Cohort 2 [rifampin]: median age, 30 years [range, 19–49 years]; male, 39%; White, 72%; BMI, 26.4 kg/m² [SD, 3.99]).⁷ In addition, the pemigatinib PBPK model was further validated by simulation of pemigatinib PK at 6, 9, 13.5, and 20 mg q.d. doses using the Simcyp virtual cancer population, with the study design matching the corresponding phase I study in adults with advanced malignancies.⁶ The simulations were performed using an age range of 21–79 years (proportion of female volunteers: 0.5), matching the demographics of the phase I study (median age, 59.0 years [range, 21.0–83.0 years]; male, 39.1%; White, 89.1%; median BMI, 27.1 kg/m² [range, 17.6–49.0 kg/m²]).⁶

Model application

Prospective prediction of other strong, moderate, and weak CYP3A4 inhibitors or inducers

The verified pemigatinib PBPK model was used to predict the effect of other strong (clarithromycin), moderate (diltiazem, erythromycin, and cyclosporine), and weak (fluvoxamine) CYP3A4 inhibitors and moderate (efavirenz) CYP3A4 inducers on pemigatinib PK. The Simcyp default PBPK models for clarithromycin, erythromycin, diltiazem, cyclosporine, fluvoxamine, and efavirenz were used in these simulations. For CYP3A4-mediated inhibition/

induction simulation, the inhibitors/inducers were administered daily from Day 1 to Day 12 and a single 13.5-mg dose of a pemigatinib tablet was administered orally on Day 8. The simulations were performed using an age range of 18–55 years (proportion of female volunteers: 0.5).

Prediction of the effect of pemigatinib on the PK of P-gp or OCT2/MATE1 substrates

The Simcyp built-in PBPK models of digoxin or metformin were used to evaluate P-gp- or OCT2/MATE1-mediated DDI for pemigatinib as inhibitor. In the simulation, pemigatinib was administered daily from Day 1 to Day 9, and a single dose of digoxin or metformin was administered orally with pemigatinib on Day 4. These simulations were performed with an age range of 18–55 years (proportion of female volunteers: 0.5).

RESULTS

PBPK model development

Simulation of pemigatinib PK

The observed and simulated mean plasma concentration–time profiles for pemigatinib following a single oral dose of pemigatinib alone in healthy volunteers (CYP3A4-mediated DDI study of pemigatinib alone)⁷ and patients with cancer (phase I dose-escalation and dose-expansion study) are shown in [Figure 1](#). Predicted and observed geometric mean plasma C_{\max} and AUC values for pemigatinib tablets are shown in [Table 2](#). For healthy volunteers, the simulated profiles of pemigatinib are very similar to the clinical data, and the predicted geometric mean C_{\max} and $AUC_{0-\infty}$ values are within 0.93- to 1.11-fold of the observed data. For patients with cancer, the simulated PK profiles of pemigatinib are comparable with the clinical data, and the predicted geometric mean C_{\max} and AUC values are within 0.610- to 1.17-fold of the observed data.

Simulation of DDI between pemigatinib and itraconazole or rifampin

The sensitivity analysis of pemigatinib $f_{mCYP3A4}$ on drug interaction with itraconazole was used to determine the CYP3A4 contribution to the metabolic clearance of pemigatinib. The input of CYP3A4 CL_{int} was varied to obtain a range of $f_{mCYP3A4}$ from 0.25 to 0.95 (using the Simcyp retrograde calculator). The simulations of itraconazole–pemigatinib DDIs with different $f_{mCYP3A4}$ values for

pemigatinib were compared with the observed DDI data. When $f_{mCYP3A4}$ was assigned to be 55%, the best prediction was achieved by the PBPK model for the effect of DDI between pemigatinib and itraconazole. Ratios of predicted and observed values of C_{\max} and AUC in the presence or absence of itraconazole or rifampin are presented in [Table 3](#). Simulated and observed plasma concentration–time profiles in the presence and absence of itraconazole or rifampin are presented in [Figure 2](#). These data have been reported previously in the European Medicines Agency Public Assessment Report for pemigatinib.¹¹ For itraconazole DDI, the pemigatinib AUC and C_{\max} ratios predicted by the model are similar to the observed values ([Table 3](#)); the predicted geometric mean AUC ratios and C_{\max} ratios are within the 90% confidence interval (CI) for the observed values. However, for rifampin DDI, AUC and C_{\max} values were underpredicted, with model-predicted pemigatinib AUC and C_{\max} ratios ~1.5- to 2-fold higher compared with the observed ratios.

PBPK model application

Simulation of pemigatinib DDI with various CYP3A4 inhibitors/inducers

The final pemigatinib PBPK model predicted the DDI from CYP3A4 inhibition well but was not able to accurately predict DDI between pemigatinib and rifampin. This could be attributed to an additional DDI effect on absorption of pemigatinib such as rifampin induction of intestinal P-gp and then decreasing of plasma concentrations of pemigatinib. The model with 55% $f_{mCYP3A4}$ was used to predict the DDI effect on pemigatinib PK when coadministered with moderate and weak CYP3A4 inducers. Results of the simulated effects of strong, moderate, and weak CYP3A4 inhibitors/inducers on pemigatinib PK are summarized in [Table 4](#) and illustrated in [Figure 3](#).

The model-simulated pemigatinib geometric mean C_{\max} and AUC ratios, respectively, for coadministration were as follows: strong inhibitor clarithromycin (1.20 and 1.89); moderate inhibitors fluconazole (1.15 and 1.83), erythromycin (1.16 and 1.66), and diltiazem (1.13 and 1.51); weak inhibitor fluvoxamine (1.05 and 1.08); and moderate inducer efavirenz (0.76 and 0.48).

Simulation of pemigatinib DDI as gut P-gp or OCT2/MATE1 inhibitors

Digoxin and metformin were used as substrates of gut P-gp and OCT2/MATE1, respectively, to evaluate the DDI for pemigatinib as a gut P-gp or OCT2/MATE1 inhibitor.

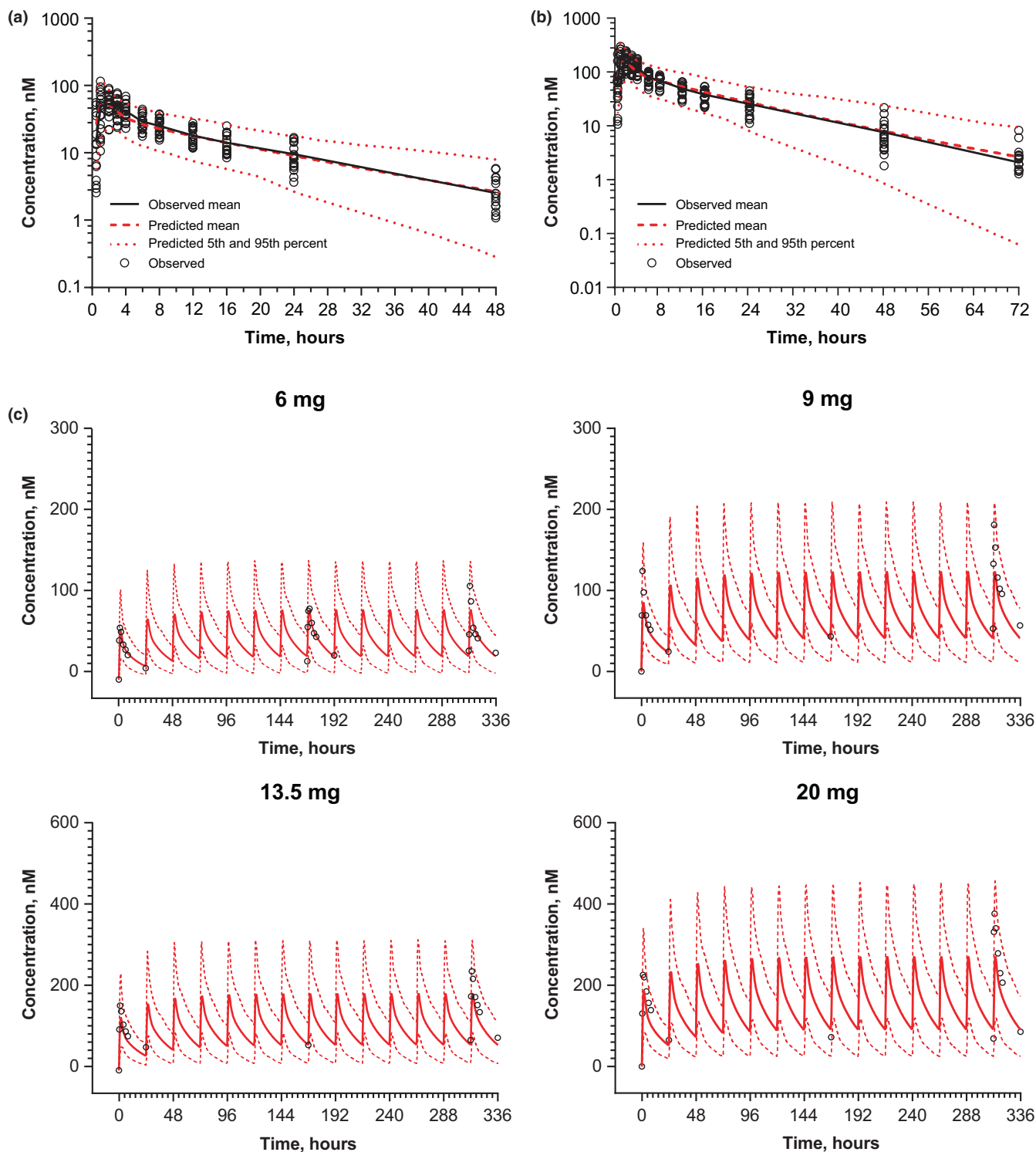


FIGURE 1 Simulated and observed mean plasma concentration–time profiles of pemigatinib: (a) single oral dose of 4.5 mg pemigatinib in the absence of itraconazole, (b) single oral dose of 13.5 mg pemigatinib in the absence of rifampin, (c) multiple oral dose (6–20 mg) of pemigatinib in patients with cancer. Simulated mean = red solid line; simulated 5% and 95% = red dashed line; observed = black circle

To confirm the Simcyp built-in PBPK model for digoxin or metformin as substrate of P-gp or OCT2/MATE1, DDI simulations between digoxin and ritonavir (Simcyp built-in model) and metformin and cimetidine (Simcyp built-in model) were performed, and simulated DDI results were

compared with clinical observation.^{12,13} Digoxin and ritonavir DDI simulation produced C_{\max} and AUC ratios of 1.39 and 1.26 for digoxin, and metformin and cimetidine DDI simulation produced C_{\max} and AUC ratios of 1.51 and 1.55 for metformin. The simulated DDI effects are

TABLE 2 Predicted and observed pemigatinib exposures (geometric mean) for single oral doses of 4.5 or 13.5 mg pemigatinib in healthy volunteers and multiple oral doses of pemigatinib in patients with cancer

Single oral dose of pemigatinib						
Dose	Predicted C_{max} (nM)	Observed C_{max} (nM)	Predicted $AUC_{0-\infty}$ (h · nM)	Observed $AUC_{0-\infty}$ (h · nM)	C_{max} (predicted/observed)	$AUC_{0-\infty}$ (predicted/observed)
4.5 mg	52.6	55.2	627	672	0.953	0.933
13.5 mg	158	176	1878	1960	0.898	0.958
Multiple oral doses of pemigatinib						
Dose	Predicted $C_{max,ss}$ (nM)	Observed $C_{max,ss}$ (nM)	Predicted $AUC_{ss,0-24}$ (h · nM)	Observed $AUC_{ss,0-24}$ (h · nM)	$C_{max,ss}$ (predicted/observed)	$AUC_{ss,0-24}$ (predicted/observed)
6 mg	77.4	78.8	1080	1050	0.982	1.03
9 mg	116	162	1259	1670	0.716	0.754
13.5 mg	193	236	3073	2620	0.818	1.17
20 mg	257	421	3345	4150	0.610	0.806

Abbreviations: AUC, area under the plasma drug concentration–time curve; $AUC_{0-\infty}$, area under the plasma concentration versus time curve integrated from start of a single dose to infinity; $AUC_{ss,0-24h}$, area under the plasma concentration versus time curve at steady-state, over one dosing interval; C_{max} , maximum plasma drug concentration; SS, steady state.

TABLE 3 Predicted and observed pemigatinib C_{max} and AUC ratios following a single oral dose of 9 mg pemigatinib tablets with and without itraconazole or rifampin administration

CYP3A4 inhibitor	C_{max} ratio		AUC ratio	
	Predicted	Observed	Predicted	Observed
Itraconazole 200 mg q.d.	1.22 (1.20–1.24)	1.17 (1.07–1.29)	1.98 (1.91–2.05)	1.88 (1.75–2.03)
Rifampin 600 mg q.d.	0.604 (0.572–0.638)	0.380 (0.332–0.425)	0.323 (0.299–0.349)	0.149 (0.139–0.161)

Note: Values are presented in the format of geometric mean (90% confidence intervals).

Abbreviations: AUC, area under the plasma drug concentration–time curve; C_{max} , maximum plasma drug concentration; CYP3A4, cytochrome P450 3A4; q.d., once daily.

comparable with observed data, indicating the Simcyp built-in PBPK model for digoxin and metformin can be used to evaluate P-gp- and OCT2/MATE1-mediated DDI.

P-gp-mediated DDI effect between digoxin and pemigatinib was evaluated using PBPK modeling with coadministration of digoxin 0.5 mg and pemigatinib 13.5 or 20 mg q.d. The simulated geometric mean ratios of C_{max} and AUC were 1.063 and 1.018 when coadministered with 13.5 mg q.d. of pemigatinib and 1.09 and 1.03 when coadministered with 20 mg q.d. of pemigatinib. Sensitivity analyses of measured K_i values for P-gp on the effect of the C_{max} and AUC ratio of digoxin were performed to further evaluate the DDI effect for pemigatinib as an inhibitor of P-gp. K_i values down to 10-fold lower than measured values ($K_i = 0.48 \mu M$) were used for sensitivity analysis. The range was 1.05–1.25 for the C_{max} ratio and 1.02–1.08 for the AUC ratio when coadministered with 13.5 mg q.d. of pemigatinib. The range was 1.07–1.29 for the C_{max} ratio and 1.02–1.10 for the AUC ratio when coadministered with 20 mg q.d. of pemigatinib.

The OCT2/MATE1-mediated DDI effect between metformin and pemigatinib was evaluated using PBPK modeling with coadministration of metformin 400 mg and pemigatinib 13.5 mg q.d. or 20 mg q.d. The simulated geometric mean ratios of C_{max} and AUC were 1.041 and 1.046 when coadministered with 13.5 mg q.d. of pemigatinib and 1.054 and 1.061 when coadministered with 20 mg q.d. of pemigatinib. A worst-case scenario simulation was performed using 10-fold lower measured K_i values ($K_{i,OCT2} = 0.0075 \mu M$ and $K_{i,MATE1} = 0.11 \mu M$) and coadministered with pemigatinib 20 mg q.d., and simulations showed C_{max} and AUC geometric mean ratios of 1.29 and 1.41, respectively.

DISCUSSION

The PK profile of pemigatinib demonstrates an approximately linear exposure to dose relationship up to 20 mg,

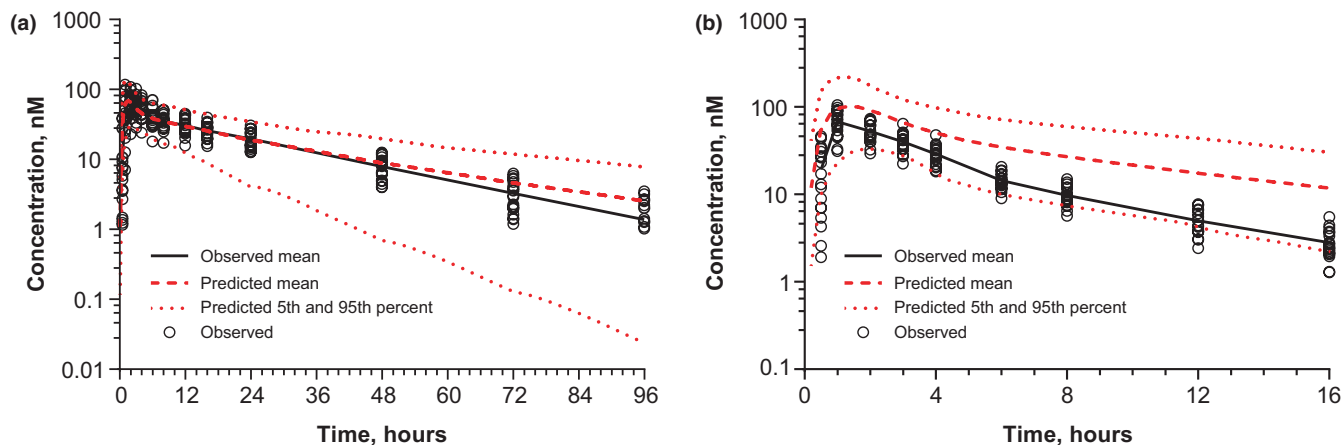


FIGURE 2 Simulated and observed plasma concentration–time profiles of a single oral dose of 9 mg pemigatinib when coadministered with (a) itraconazole (200 mg once daily [q.d.]) and (b) rifampin (600 mg q.d.)

TABLE 4 Simulated pemigatinib drug–drug interactions with various CYP3A4 inhibitors or inducers

CYP3A4 perpetrators and dose regimen	Inhibition/induction mechanism	AUC ratio, geometric mean (90% confidence interval)	C_{\max} ratio, geometric mean (90% confidence intervals)
Itraconazole 200 mg q.d.	Strong, reversible inhibition	1.98 (1.91–2.05)	1.22 (1.20–1.24)
Clarithromycin 500 mg b.i.d.	Strong, time-dependent inhibition	1.89 (1.80–1.98)	1.20 (1.18–1.21)
Fluconazole 400 mg q.d.	Moderate, reversible inhibition	1.83 (1.78–1.90)	1.15 (1.13–1.16)
Erythromycin 500 mg b.i.d.	Moderate, time-dependent inhibition	1.66 (1.59–1.73)	1.16 (1.14–1.17)
Diltiazem 60 mg t.i.d.	Moderate, time-dependent inhibition	1.51 (1.46–1.56)	1.13 (1.12–1.14)
Fluvoxamine 50 mg q.d.	Weak, reversible inhibition	1.08 (1.08–1.09)	1.05 (1.04–1.05)
Rifampin 600 mg q.d.	Strong inducer	0.323 (0.299–0.349)	0.604 (0.572–0.638)
Efavirenz 600 mg q.d.	Moderate inducer	0.482 (0.455–0.512)	0.758 (0.736–0.781)

Note: Values are presented in the format of geometric mean (90% confidence intervals).

Abbreviations: AUC, area under the plasma drug concentration–time curve; b.i.d., twice daily; C_{\max} , maximum plasma drug concentration; CYP3A4, cytochrome P450 3A4; q.d., once daily; t.i.d., three times daily.

the highest dose studied. Pemigatinib is eliminated predominantly through hepatic metabolism, whereas the contribution from renal excretion is minimal. The in vitro data suggest that the CYP3A4 plays a primary role in the metabolic clearance of pemigatinib. A clinical DDI study⁷ with itraconazole and rifampin confirmed that pemigatinib is a CYP3A4 substrate (AUC ratios of 1.88 and 0.149, respectively).

The PBPK model for pemigatinib was initially built using in vitro and physicochemical data. Then a minimal PBPK with an ADAM absorption model for pemigatinib that incorporates CYP3A4-mediated metabolism derived from in vitro data, mass balance data, and clinical PK data was developed. The pemigatinib PBPK model-predicted PK profiles describe the clinical data in healthy volunteers appropriately. Furthermore, the PBPK model-predicted PK profiles in patients with cancer describe the clinical data well. The contribution of CYP3A4 to the metabolic

clearance ($f_{mCYP3A4}$) was first estimated by a sensitivity analysis of pemigatinib $f_{mCYP3A4}$ on drug interaction with itraconazole, and it was further confirmed to be 0.55 by matching the simulated PK profiles of pemigatinib with or without coadministration of itraconazole to clinical DDI data. The metabolism and elimination of pemigatinib have been extensively evaluated in the human ADME study as well as a battery of in vitro studies. As noted in our previous work,¹⁴ in the human ADME study (unpublished data), 72% of the total radioactivity was accounted for by known metabolites; 76.9% of the metabolite burden in urine and feces was derived from M2 (O-desmethyl-pemigatinib) and its secondary metabolites. In vitro metabolism studies show that CYP3A4 is solely responsible for M2 formation from pemigatinib. Therefore, it is unlikely that there is yet another metabolic pathway that is responsible for >25% of total clearance of pemigatinib. The predicted geometric mean AUC ratio and C_{\max} ratio

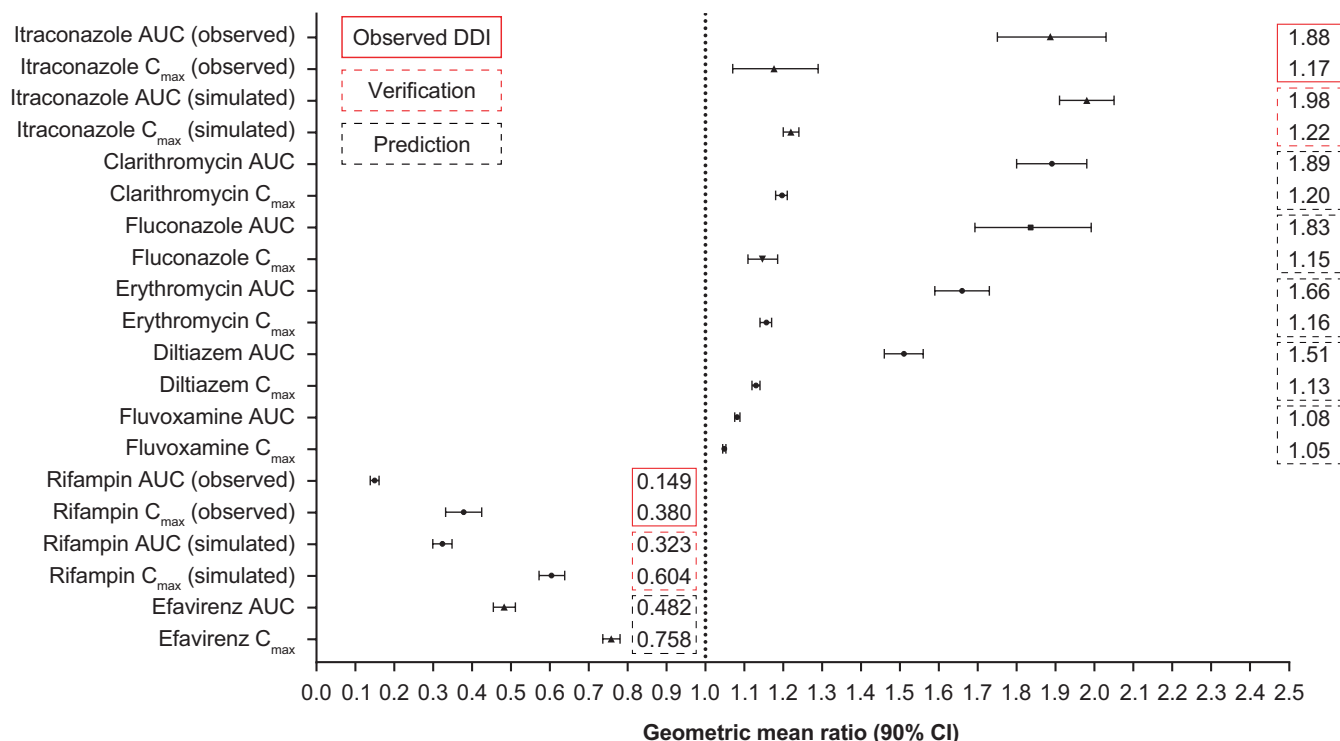


FIGURE 3 Observed and simulated AUC and C_{max} ratios of a single dose of 13.5 mg pemigatinib with various cytochrome P450 3A4 inhibitors and inducers. AUC, area under the plasma drug concentration–time curve; C_{max}, maximum plasma drug concentration; CI, confidence interval; DDI, drug–drug interaction

are within the 90% CI of the observed data for itraconazole DDI. However, underprediction is observed for rifampin DDI, and the model-predicted pemigatinib AUC and C_{max} ratios are ~1.5- to 2-fold higher compared with the observed AUC and C_{max} ratios for rifampin DDI. In the CYP3A4-mediated DDI study, an 85% reduction in AUC and 63% decrease in half-life of pemigatinib were observed following rifampin coadministration. In addition, the first-pass gut and liver metabolism is expected to be low as simulated in this PBPK model because of the high permeability and low oral clearance of pemigatinib. All of these suggest that a decrease in bioavailability of pemigatinib occurred with rifampin coadministration in addition to an increase in systemic clearance (e.g., rifampin decreases pemigatinib absorption by induction of intestinal P-gp¹⁵).

The retrospective PBPK model simulation of the CYP-mediated DDIs using the observed clinical DDI data-validated PBPK model has been recognized as a useful tool for predicting the DDI with other CYP inhibitors or inducers.^{16,17,18} The model predicted a >50% AUC increase for coadministration with either strong or moderate CYP3A4 inhibitors, which is beyond the highest clinically explored exposures at 20 mg q.d. Therefore, pemigatinib dose reduction is required when coadministered with strong or moderate CYP3A4 inhibitors. No DDI is predicted between

pemigatinib and a weak CYP3A4 inhibitor. However, a limitation to this study is that the final pemigatinib PBPK model was not able to accurately predict DDI between pemigatinib and rifampin, which could be attributed to additional DDI effects on the absorption of pemigatinib; the complexity associated with the disposition of rifampin and subsequent impact of those factors on DDI with rifampin are acknowledged in the literature.¹⁹ As such, it would be appropriate to identify other prototypical CYP3A4 inducers in place of rifampin in the future.²⁰

The model with 55% $f_{mCYP3A4}$ predicted a >50% AUC decrease for coadministration with either strong or moderate CYP3A4 inducers. Therefore, coadministration of strong or moderate CYP3A4 inducers should be avoided. In addition, itraconazole increased pemigatinib exposure by about 90%, suggesting that pemigatinib is not a sensitive substrate. Therefore, the effect of a weak CYP3A4 inducer (such as dexamethasone) on pemigatinib is expected to be small.

The worst-case scenario DDI simulation for pemigatinib as an inhibitor of P-gp or OCT2/MATE1 substrates using 10-fold lower measured K_i values showed a modest DDI effect (1.25-fold C_{max} and 1.41-fold AUC increase for digoxin and metformin, respectively), suggesting no dose adjustment for pemigatinib when coadministered with P-gp or OCT2/MATE1 substrates.

CONCLUSIONS

The PBPK modeling and simulation predicted itraconazole DDI appropriately, but could not recover the rifampin DDI data. The validated pemigatinib PBPK model was used to evaluate other CYP3A4 inhibitors/inducers to support the label and provide dose recommendations for clinical trials. The simulation results indicate that coadministration with strong or moderate CYP3A4 inhibitors should be avoided, which supports the approved label for pemigatinib²; if unavoidable, the dose should be reduced from 13.5 to 9 mg or from 9 to 4.5 mg. No dose adjustment is required for coadministration of pemigatinib with weak CYP3A4 inhibitors. The current model with 55% $f_{mCYP3A4}$ predicted a >50% pemigatinib AUC decrease for coadministration with strong and moderate CYP3A4 inducers. Therefore, coadministration of strong or moderate CYP3A4 inducers should be avoided, which supports the approved label for pemigatinib.² The evaluation of pemigatinib as a P-gp or OCT2/MATE1 inhibitor using the pemigatinib PBPK model suggests that pemigatinib can be coadministered with P-gp or OCT2/MATE1 substrates without any dose adjustment.

ACKNOWLEDGMENTS

Scientific contributions by Ruth-Young Sciamé, Yan Zhang, Kwang-Jong Chen, and Stephanie Wezalis toward generating in vitro metabolism and transporter interaction data are acknowledged. The authors thank the patients and their families, the investigators, and the site personnel who participated in these studies. Editorial assistance was provided by Envision Pharma Group, Inc. (Philadelphia, PA), and funded by Incyte Corporation.

CONFLICT OF INTEREST

Tao Ji is a former employee and shareholder of Incyte Corporation. Xuejun Chen and Swamy Yeleswaram are employees and shareholders of Incyte Corporation.

AUTHOR CONTRIBUTIONS

T.J. wrote the manuscript. T.J., X.C., and S.Y. designed the research, performed the research, and analyzed the data.

REFERENCES

- Liu PCC, Koblisch H, Wu L, et al. INCB054828 (pemigatinib), a potent and selective inhibitor of fibroblast growth factor receptors 1, 2, and 3, displays activity against genetically defined tumor models. *PLoS One*. 2020;15:e0231877. doi:10.1371/journal.pone.0231877
- PEMAZYRE™ (pemigatinib) tablets [prescription information]. Incyte Corporation; 2021.
- Pemazyre (Pemigatinib) [Product Information]. Incyte Biosciences Distribution B.V.; 2021.
- Pemazyre (ペマジール) [pemigatinib (ペミガチニブ)] tablets; Package Insert. Incyte Corporation; 2021.
- Incyte Announces Health Canada Conditional Approval of Pemazyre (pemigatinib) as First Targeted Treatment for Adults with Previously Treated, Unresectable Locally Advanced or Metastatic Cholangiocarcinoma. Incyte Corporation; 2021.
- Subbiah V, Iannotti NO, Gutierrez M, et al. FIGHT-101, a first-in-human study of potent and selective FGFR 1-3 inhibitor pemigatinib in pan-cancer patients with FGF/FGFR alterations and advanced malignancies. *Ann Oncol*. 2022;33:522-533. doi:10.1016/j.annonc.2022.02.001
- Ji T, Rockich K, Epstein N, et al. Evaluation of drug–drug interactions of pemigatinib in healthy participants. *Eur J Clin Pharmacol*. 2021;77:1887-1897. doi:10.1007/s00228-021-03184-z
- US Food and Drug Administration. Guidance for industry: in vitro drug interaction studies — cytochrome p450 enzyme- and transporter-mediated drug interactions. 2020.
- Ji T, Lihou C, Asatiani E, et al. Pharmacokinetics and pharmacodynamics of pemigatinib, a potent and selective inhibitor of FGFR 1, 2, and 3, in patients with advanced malignancies. *Mol Cancer Ther*. 2019;18(12 Suppl):C071. doi:10.1158/1535-7163.TARG-19-C071
- Zhou W, Johnson TN, Xu H, et al. Predictive performance of physiologically based pharmacokinetic and population pharmacokinetic modeling of Renally cleared drugs in children. *CPT Pharmacometrics Syst Pharmacol*. 2016;5:475-483. doi:10.1002/psp4.12101
- Pemazyre (pemigatinib) [assessment report]. Incyte Biosciences Distribution B.V.; 2021.
- Penzak SR, Shen JM, Alfaro RM, Remaley AT, Natarajan V, Falloon J. Ritonavir decreases the nonrenal clearance of digoxin in healthy volunteers with known MDR1 genotypes. *Ther Drug Monit*. 2004;26:322-330. doi:10.1097/00007691-200406000-00018
- Somogyi A, Stockley C, Keal J, Rolan P, Bochner F. Reduction of metformin renal tubular secretion by cimetidine in man. *Br J Clin Pharmacol*. 1987;23:545-551. doi:10.1111/j.1365-2125.1987.tb03090.x
- Ji T, Chen X, Liu X, Yeleswaram S. Population pharmacokinetics analysis of pemigatinib in patients with advanced malignancies. *Clin Pharmacol Drug Dev*. 2022;11:454-466. doi:10.1002/cpdd.1038
- Greiner B, Eichelbaum M, Fritz P, et al. The role of intestinal P-glycoprotein in the interaction of digoxin and rifampin. *J Clin Invest*. 1999;104:147-153. doi:10.1172/JCI6663
- Budha NR, Ji T, Musib L, et al. Evaluation of cytochrome P450 3A4-mediated drug–drug interaction potential for cobimetinib using physiologically based pharmacokinetic modeling and simulation. *Clin Pharmacokinet*. 2016;55:1435-1445. doi:10.1007/s40262-016-0412-5
- Templeton I, Ravenstijn P, Sensenhauser C, Snoeys J. A physiologically based pharmacokinetic modeling approach to predict drug–drug interactions between domperidone and inhibitors of CYP3A4. *Biopharm Drug Dispos*. 2016;37:15-27. doi:10.1002/bdd.1992
- Yoshida K, Budha N, Jin JY. Impact of physiologically based pharmacokinetic models on regulatory reviews and product labels: frequent utilization in the field of oncology. *Clin Pharmacol Ther*. 2017;101:597-602. doi:10.1002/cpt.622
- Almond LM, Mukadam S, Gardner I, et al. Prediction of drug–drug interactions arising from CYP3A induction using a physiologically based dynamic model. *Drug Metab Dispos*. 2016;44:821-832. doi:10.1124/dmd.115.066845

20. Srinivas NR. Pharmacokinetic interaction of rifampicin with oral versus intravenous anticancer drugs: challenges, dilemmas and paradoxical effects due to multiple mechanisms. *Drugs R D*. 2016;16:141-148. doi:[10.1007/s40268-016-0133-0](https://doi.org/10.1007/s40268-016-0133-0)

SUPPORTING INFORMATION

Additional supporting information may be found in the online version of the article at the publisher's website.

How to cite this article: Ji T, Chen X, Yeleswaram S. Evaluation of drug–drug interaction potential for pemigatinib using physiologically based pharmacokinetic modeling. *CPT Pharmacometrics Syst Pharmacol*. 2022;11:894-905. doi: [10.1002/psp4.12805](https://doi.org/10.1002/psp4.12805)